



Laser catalysis of acrylonitrile on copper surfaces

J.O. Cáceres¹, J. Tornero López, A. González Ureña*

*Unidad de Láseres y Haces Moleculares, Instituto Pluridisciplinar, Universidad Complutense de Madrid, Juan XXIII,
E-28040 Madrid, Spain*

Received 12 November 1999; in final form 7 March 2000

Abstract

The electron emission and CN^- yield produced by laser irradiation of acrylonitrile (ACN) adsorbed on a polycrystalline Cu surface have been investigated over the $930\text{--}953\text{ cm}^{-1}$ wavenumber range. Both emissions show a clear wavelength dependence with a ca. 20 cm^{-1} red shift with respect to the gas-phase ACN spectrum. The laser catalysis CN^- yield is discussed in light with both substrate and adsorbate-mediated mechanisms, which seem to be controlling this (charge-transfer) surface reaction. © 2000 Elsevier Science B.V. All rights reserved.

1. Introduction

Photon beams, particularly intense lasers, have been extensively used in recent years to induce or enhance chemical interaction at gas–solid interfaces [1,2]. Both the basic scientific interest and the technological application in material processing for new materials drive the rapid expansion of the field, which can be generally referred to as laser-induced gas–surface chemistry [2–5].

Electronic relaxation on metal surfaces is extremely rapid and consequently, many of the surface reactions promoted by laser irradiation on metal substrates in contact with optically non-absorbing gases are often interpreted as thermally activated processes. This is the case of IR-induced desorption

in which the thermal (photodesorption) mechanism, due to resonant substrate heating [6–8], seems to be well accepted [8]. There is, however, an increasing evidence that non-thermal photochemical processes play an important role in certain gas–surface systems when resonant IR radiation is used [9–11].

Thus, the surface femtochemistry of O_2 and CO on Pt(111) has been investigated with the finding that non-thermal electron distributions play a significant role in both O_2 desorption and CO_2 formation [9]. More recently, the desorption and oxidation of CO on Ru (0001) have been investigated with femtosecond IR laser pulses [12]. This study led to the interesting conclusion that while CO desorption is caused by a phonon-mediated mechanism, the CO oxidation to CO_2 product was initiated by hot substrate electrons.

In the present work, as the laser pulse duration (see below) is of the order of microseconds both electrons and phonons are in equilibrium and only thermal surface chemistry should be, in principle,

* Corresponding author. Fax: +34-91-3943265; e-mail: laseres@eucmax.sim.ucm.es

¹ CONICET postdoctoral fellow.

expected [13]. Nevertheless, the possibility of some non-thermal effects, i.e. that other parameters, in addition to the temperature, play a role in the surface chemistry, cannot be ruled out. This could be the case for substrate–adsorbate charge transfer reactions in which the (adsorbate) dissociative electron attachment rate is fast enough to be competitive with energy redistribution among the vibrational modes of the adsorbate following laser excitation. Under these conditions, in spite of the fast electron relaxation to a thermal (Fermi–Dirac) distribution and the adsorbate–substrate energy transfer, some vibrational selectivity may be retained when local mode excitation changes the adsorbate electron affinity, and so the barrier for its electron attachment, at a rate faster or comparable to that of adsorbate vibrational energy redistribution. These conditions would then originate a selective chemistry with a different reaction yield from that of the non-selective case, in which only an enhanced heating, upon vibrational excitation of the adsorbate, would take place. The criterion that excitation energy must remain relatively localized during the reaction in order to achieve mode-selective chemistry is well established for many fast direct reactions [14]. We anticipate that this seems to be the case for the laser-induced dissociative ionization of acrylonitrile (C_3H_3N or vinylcyanide), denoted by ACN hereafter, adsorbed on copper as investigated here.

The present work reports on the investigation of laser-induced ionisation processes at the gas–surface interface using a TEA– CO_2 laser for the excitation of molecules. The surface used was polycrystalline Cu, which has a rather low work function (4.64 eV) [15]. The adsorbate was the acrylonitrile molecule (electron affinity 1.247 eV) [15], which strongly absorbs in the ν_{13} band associated with the RCH–CN bond resonant with transitions between 954.55 and 931.00 cm^{-1} corresponding to the 10P(8) and 10P(34) lines of the CO_2 laser [16], respectively.

Our main motivation was to look for gas–surface ionization processes induced by laser radiation. Thus, the experiment is aimed at investigating the parent or any fragment ion yield as a function of the laser wavelength and power as well as other surface parameters, which characterize the gas–surface interaction, in a search for vibrationally enhanced effects in the acrylonitrile dissociative attachment.

2. Experimental

The experimental setup is schematically shown in Fig. 1. The main parts of it are: (a) the line-tunable IR CO_2 laser focused on the Cu surface, (b) the argon ion gun for cleaning the surface and (c) the linear time-of-flight mass spectrometer (TOFMS).

Experiments were performed with an IR TEA– CO_2 laser (Coherent Hull XL-370 TS), which can be tuned over the 9–11 μm wavelength range. The laser enters in an ultrahigh vacuum chamber (UHVC) in which a mechanically polished polycrystalline copper surface (99.9998% Aldrich Chemical) was allocated. The typical laser spot area on the surface was 0.05 cm^2 . A pure TEM_{00} mode was always used for all wavelengths. Under the present conditions, the surface temperature, estimated with the model developed by Burgess [17] never exceeded 810 K. In addition, careful monitoring of both spatial distribution and temporal profile of laser pulses revealed the absence of hot spots. A spectrum analyzer (Macken Instrument model 16-A.) was used to tune the laser to the desired wavelength. An Ar ion gun (VG Microtech Instruments model AG5000, 5 keV ions sputtering at 298 K) cleaned the surface before each experiment. The cleanliness of the Cu surface was

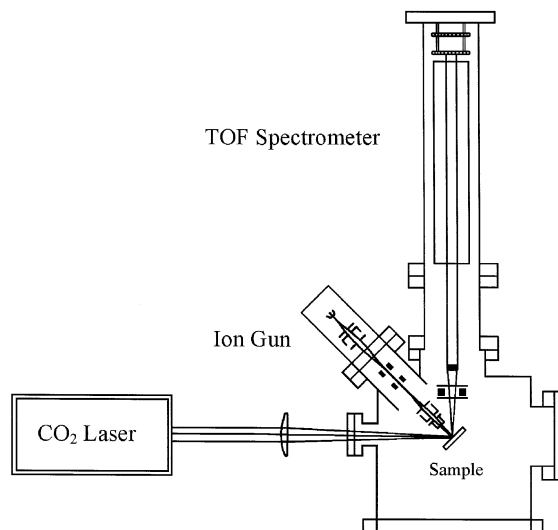


Fig. 1. Schematic view of the experimental setup including the CO_2 laser, Ar ion gun and TOFMS.

Table 1
Experimental conditions

Laser system

Wavelength range: 9–11 μm
 Typical fluence: $\approx 4 \text{ J/cm}^2$
 Temporal profile per pulse: FWHM peak 100 ns (tail 3 μs)
 Pulse frequency: 2 Hz
 Spot size: 0.05 cm^2

Vacuum

Background pressure: $\leq 3 \times 10^{-9}$ Torr
 Acrylonitrile range pressure: 2.0×10^{-8} to 2.0×10^{-7} Torr
 Copper temperature: 300 K
 Surface cleaning: 5 keV ion sputtering with Ar ion gun

checked by detection of impurities in the TOF signal. No negative or positive ion desorption was observed from the clean Cu surface for laser fluences of the order of 4 J/cm^2 , which was the typical value used.

The Cu surface can be heated resistively by a nicrom wire up to 675 K. This heat treatment was employed to eliminate surface impurities because they may alter the electronic properties of the surface and, consequently, the negative ion yield.

Acrylonitrile (99 + % Aldrich Chemical) is a colorless liquid at room temperature and atmospheric pressure, therefore volatile impurities were removed from the samples through freeze and thaw cycles. Gas chromatographic analyses and IR spectroscopy showed the absence of impurities in the ACN sample. During the experiments the acrylonitrile pressure was kept at 5.0×10^{-8} Torr. Since the laser repetition rate was 2 Hz, the acrylonitrile exposure during the laser shot interval was 0.025 L ($1 \text{ L} = 1 \times 10^{-6}$ Torr s).

A 50 cm linear TOFMS mounted with a dual microchannel plate (MCP) detector (Comstock CP-625C/50F) and optimized for negative ion detection was used. The signal was then further amplified with an oscilloscope Tektronix (TDS 540) and finally stored and processed in a computer. When the signal-to-noise demanded better resolution or discrimination, a multichannel signal averager (Stanford Research System) was used to obtain the TOF spectra. Typically the average of 100 TOF spectra resulted in good statistics. Table 1 lists the most relevant experimental parameters and conditions of the present work.

3. Results

The appearance of a CN^- peak in the TOF spectrum when ACN is introduced in the vacuum chamber and adsorbed on the surface is noticeable as is displayed in Fig. 2. This spectrum persisted after the ACN leak was closed and the background pressure reached the low 10^{-9} Torr range. The top figure shows the same spectrum obtained before the ACN was added. Only the fast electron signal can be seen. For a better illustration the inset shows a typical TOF spectrum of the electron signal together with that of the laser pulse.

Both CN^- and electron signals were monitored at different wavelengths between 953 and 930 cm^{-1} at constant laser fluence. Fig. 3 shows the wavelength

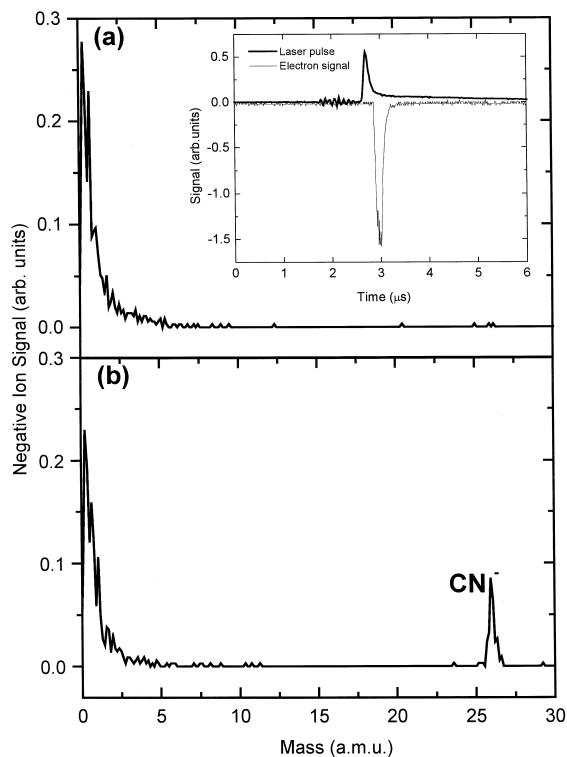


Fig. 2. Negative ion TOF spectra obtained at 3×10^{-9} Torr of background pressure and rest of conditions specified in Table 1 with a laser excitation wavenumber of 945.48 cm^{-1} . (a) Only the electron signal is present with no ACN added. The inset shows a typical electron TOFMS signal (bottom) with the laser signal incorporated (top) for a better illustration. (b) Same as in (a) but with ACN added ($p_{\text{ACN}} \approx 10^{-8}$ Torr).

dependence of the integrated signals. It can be seen (Fig. 3a) that the maximum CN^- signal is obtained for the 10P32 laser line (933.7 cm^{-1}) which also corresponds to the maximum electron yield (Fig. 3b) when acrylonitrile is present. With no acrylonitrile, a random dispersion around a constant value indicates no wavelength dependence for the emitted electrons as depicted in Fig. 3c.

Fig. 3b,c have the same arbitrary units for the electron signal. The constant value (within experi-

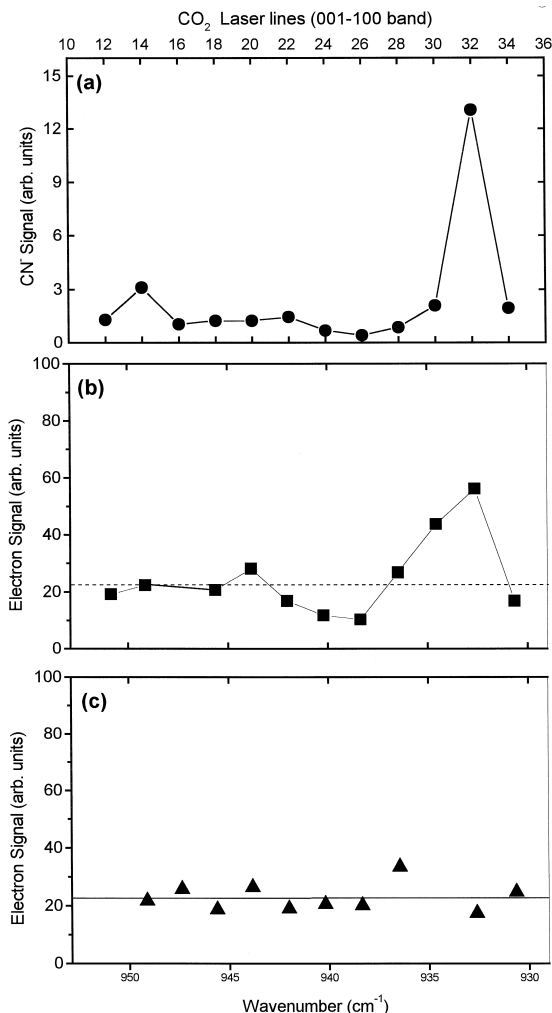


Fig. 3. Electron and CN^- signal wavelength dependence for a fixed laser fluence: (a) CN^- spectrum obtained at a $p_{\text{ACN}} = 3 \times 10^{-8}$ Torr. (b) Electron signal spectrum obtained at same conditions as in (a). (c) Same as in (b) but with no ACN pressure added: notice the clear wavelength dependence in both top and middle panels which, in turn, is absent in the bottom spectrum.

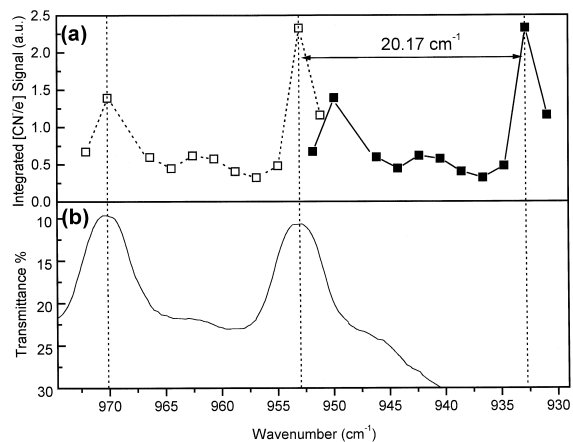


Fig. 4. (a) Solid square: CN^-/e^- signal ratio as a function of the laser wavenumber. Open square. Same as before, but shifted 20.17 cm^{-1} to the blue part of the spectrum. In both cases a solid (dashed) line was drawn through the points to guide the eye. (b) IR ACN gas-phase spectrum. Vertical dashed lines are drawn through the peaks to reinforce the similarity between these two spectra.

mental error) of the electron signal in the absence of ACN (solid line of Fig. 3c) has also been marked by a dashed-line in Fig. 3b. Thus, except for the red part of the spectrum, a small decrease in the electron yield can be noticed when ACN is added.

A closer look at the red part of the spectrum suggests a correlation between both CN^- and electron signals. Indeed, measuring the total CN^- and the electron signal dependence on laser fluence, a linear correlation (not shown) between them was always found for all wavelengths. Nevertheless, the CN^- signal normalized by the electron yield, i.e. the CN^-/e^- ratio still retains a clear wavelength dependence as displayed in the upper part of Fig. 4. On the other hand, it is interesting to point out the close resemblance between the present CN^-/e^- spectrum and the ACN gas-phase absorption spectrum shown in the lower part of the same figure. Moreover, a red shift of ca. 20 cm^{-1} , as indicated, should be remarked.

4. Discussion

The observation of a CN^- peak in the TOF spectrum proves the occurrence of ACN dissociative attachment induced by laser radiation. Furthermore,

the wavelength dependence, even in the CN^-/e^- ratio, clearly indicates the signature of the ACN resonant vibrational absorption. The 970 and 953 cm^{-1} peaks of the ACN gas-phase absorption spectrum are assigned to the ($=\text{CHCN}$) and ($=\text{CH}_2$) wagging modes [16], respectively. The red shift of ca. 20 cm^{-1} observed in the CN^-/e^- spectrum could be due either to the presence of gas-phase multiphoton absorption leading to ACN dissociative attachment or to the weakening of the molecular bond typically associated to the bond formation between the adsorbate and the metal surface [18].

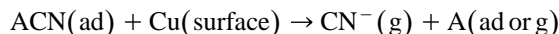
There are several arguments and observations that run against the gas-phase dissociative attachment mechanism, i.e. schematically: $\text{ACN}^\dagger + \text{e}^- \rightarrow \text{A} + \text{CN}^-$. These are the following.

1. *Energetics*: This process is very endoergic as ΔH_0° is given by $\Delta H_0^\circ = D_0^\circ(\text{A-CN}) - \text{EA}(\text{CN}) = 5.66 \text{ eV}$ (Ref. [19]) $- 3.83 \text{ eV}$ (Ref. [15]) $= 1.83 \text{ eV}$. A simple estimate of the average kinetic energy of the emitted electrons, E_e , gives $E_e < 10 \text{ meV}$ which by energy balance requires a minimum ACN internal energy excitation of 1.82 eV to overcome the dissociative attachment barrier. This energy barrier would correspond to ca. 16 photons of 933 cm^{-1} . By contrast the measured CN^-/e^- signal versus laser fluence (not shown) showed zero slope.
2. *Electron yield dependence on laser frequency*: The gas-phase attachment mechanism does not explain the electron yield dependence on laser frequency observed in Fig. 3 (middle panel) which was measured at constant laser fluence. Such a 'resonant' enhancement of the electron yield necessarily implies a gas-surface or adsorbate-substrate interaction.

In line with above considerations a crucial question to be considered is whether the $\text{ACN}(\text{g}) + \text{Cu}(\text{s})$ collisions is the limiting step of the observed electron and CN^- ions. Under the present pressure conditions ($p = 10^{-7}$ Torr) the number of gas-surface collisions is about 2×10^{11} collisions $\text{cm}^{-2} \text{ s}^{-1}$. Thus, considering a Cu density of 10^{14} atoms cm^{-2} every surface Cu atom collides with an ACN molecule within

$$\tau = \frac{10^{14}}{2 \times 10^{11}} \approx 5000 \text{ s collision}^{-1}.$$

Obviously, the observation of a much shorter TOF for electrons (0.3 μs) and CN^- ions (10.5 μs) precludes the gas-surface collision as the limiting step of the charge transfer process. In other words, the observed electrons and CN^- must be produced in a much faster process, as the ACN surface dissociative attachment, i.e.



which can take place via the following two modalities.

1. *Substrate-mediated absorption*. Essentially the laser radiation heats the electron in the substrate pumping them out of the Fermi level and subsequently they tunnel to the ACN^- potential which leads to $\text{A} + \text{CN}^-$ products. This process is schematically shown in the top panel of Fig. 5 for a better illustration. Obviously, this mechanism would show a thermal character without significant frequency selectivity.
2. *Adsorbate-mediated absorption*. In this case, the vibrational absorption of the ACN molecule is predominant. This may have several consequences: first an enhanced local heating of the surface electrons and therefore an enhanced realisation of the first mechanism with the corresponding increase of the electron yield. Secondly, an increase in the CN^- yield due to a lowering of the ΔE value (see bottom panel of Fig. 5). Now the value of ΔE could be lower than ΔH_0° since: (i) the ACN is adsorbed on the Cu surface and presumably the $\text{CH}_2\text{C-CN}$ bond is softer. (ii) the resonant vibrational absorption increases the molecular electron affinity and so it facilitates the electron attachment.

In principle, due to the thermal mechanism expected upon the microsecond timescale of the laser excitation, the enhancement of the CN^- ion and electron yield would be caused by additional heating of the system though resonant absorption of light by excitation of the ACN vibration. In this view, the local vibrational mode would only function as an antenna for the gathering of heat. If we consider that while free electron formation requires electrons with energy above 4.6 eV (i.e. just to surmount the work function barrier) and that CN^- formation only electrons with energy above 1.8 eV (i.e. the work function barrier minus the CN electron affinity) the

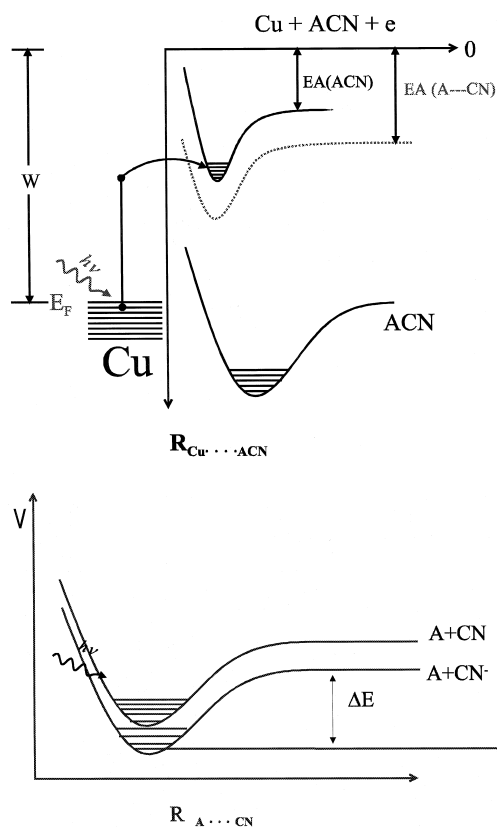


Fig. 5. Top: idealized one-dimensional potential energy for the ACN/Cu system. Both neutral Cu...ACN and negative Cu...ACN⁻ potentials are displayed. Here W, E_F and EA stand for work function, Fermi energy level and electron affinity, respectively. Dashed line represents the same Cu...ACN⁻ potential, but for an increased A...CN⁻ distance and so higher electron affinity (EA_{ACN}) at the asymptotic limit. The electron pumps out of the Fermi level upon laser excitation and subsequent tunnelling takes place. See text for comments. At the bottom part of the figure the neutral covalent and ionic A...CN potentials are qualitatively shown in which the asymptotic energy difference is given by $\Delta E = D_0^0(A-CN) - EA(CN)$. See text for comments.

CN⁻/e⁻ branching ratio will then be proportional to exp. $((4.6-1.8) \text{ eV}/kT)$. Here k is the Boltzmann constant and T the temperature. This ratio decreases with temperature contrary to that experimentally observed. This discrepancy indicates that all observations cannot be explained assuming thermal equilibrium. In other words, other parameters, in addition to the temperature, should play a role in the surface chemistry.

Since the dissociative attachment of the (adsorbed) ACN should also depend on its electron affinity, the observed enhancement in the CN⁻/e⁻ ratio could be due to the lowering of the dissociative electron attachment barrier such that a vibrationally selective chemistry cannot be completely ruled out. In this picture, the ACN vibrational mode would function not only as an antenna for increasing the metal temperature, but it would also introduce some selectivity by reducing the surface reaction barrier due to the enhanced adsorbate electron affinity. In this picture, the resonant excitation remains localized during the very fast dissociative attachment process such that subsequent energy transfer from the excited adsorbate into dissipative channels is not comparable to the rate of formation of the CN⁻ moiety.

In view of all the above arguments and the whole body of data, both possibilities, i.e. substrate- and adsorbate-mediated absorption may be present as the laser radiation is focused onto the surface. Obviously, pump and probe femtosecond experiments carried out on this system would provide an experimental real-time confirmation of the suggested dynamical picture for the acrylonitrile catalysis on copper investigated here.

5. Conclusions

The main conclusions to be drawn from this investigation are the following.

1. Important catalytic effects can be achieved by laser-induced dissociative attachment of ACN on Cu surfaces leading to CN⁻ as the main product.
2. Both substrate and adsorbate mediated mechanisms seem to be controlling the charge transfer surface reactions. Indeed, a clear enhancement in both electron and CN⁻ signals is obtained by resonant excitation of the adsorbate vibrational modes.
3. The wavelength dependence of the CN⁻/e⁻ branching ratio suggests the possibility of some vibrational selectivity controlling the yield of this surface electron attachment chemical reaction.

Finally, the present results provide a new insight not only into the dynamics of gas-surface interactions but also into new routes for industrial applications of chemical processes. With regard to the

former it would be interesting to perform this type of investigation using ultrafast femtosecond laser excited surface reactions. It could unambiguously differentiate the thermal from the vibrationally selective mechanisms that seem to be present in this surface reaction.

Acknowledgements

Financial support from DGES of Spain Grant PB97-0272 and Ramon Areces Foundation is gratefully acknowledged.

References

- [1] T.J. Chuang, Surf. Sci. Rep. 3 (1983) 105.
- [2] T.J. Chang, Surf. Sci. 178 (1986) 763.
- [3] W. Zhang, P.G. Smirniotis, J. Catal. 182 (1999) 70.
- [4] J. Kubota, J. Kondo, K. Domen, C. Hirose, J. Elec. Spectrosc. 64/65 (1993) 163.
- [5] J. Castaño, V. Zapata, G. Makarov, A. González Ureña, J. Phys. Chem. 99 (1995) 13659.
- [6] I. Hussla, H. Seki, T.J. Chuang, Z.W. Gortel, H.J. Kreuzer, P. Piercy, Phys. Rev. B 32 (1985) 3498.
- [7] A. Dereux, A. Peremans, J.-P. Vigneron, J. Darville, J.M. Gilles, J. Electron Spectrosc. Relat. Phenom. 45 (1987) 261.
- [8] A. Peremans, A. Dereux, F. Maseri, J. Darville, J.M. Gilles, J.-P. Vigneron, Phys. Rev. B 45 (1992) 8598.
- [9] M.E. Umstead, M.C. Lin, J. Phys. Chem. 82 (1978) 2047.
- [10] I. Her, R.J. Finlay, C. Wu, E. Mazur, J. Chem. Phys. 108 (1998) 8595.
- [11] S. Delivala, R.J. Finlay, J.R. Goldman, T.H. Her, W.D. Mieher, E. Mazur, Chem. Phys. Lett. 242 (1995) 617.
- [12] M. Bonn, S. Funk, Ch. Hess, D.N. Denzler, C. Stampfl, M. Scheffler, M. Wolf, G. Ertl, Science 285 (1999) 1042.
- [13] J.W. Gadzuk, in: J. Manz, L. Wöste (Eds.), Femtosecond Chemistry, Chap. 20, Vol. 2, VCH, Weinheim, 1995.
- [14] R.N. Zare, Science 279 (1998) 1875.
- [15] Handbook of Chemistry and Physics, 74rd edn., 1993–1994.
- [16] M. Khelifi, M. Nollet, P. Paillous, P. Bruston, F. Raulin, Y. Bénilan, R.K. Khanna, J. Mol. Spectrosc. 194 (1999) 206.
- [17] D. Burgess Jr., P.C. Stair, E. Weitz, J. Vac. Sci. Technol. A 4 (1986) 1362.
- [18] J.K. Norskov, Rep. Prog. Phys. 53 (1990) 1253, See for example.
- [19] S.W. North, G.E. Hall, Chem. Phys. Lett. 263 (1996) 148.